Available online at www.sciencedirect.com
ScienceDirect
Polymer 48 (2007) 229–238
polymer
www.elsevier.com/locate/polymer

A solid-state and suspended-state magic angle spinning nuclear magnetic resonance spectroscopic investigation of a 9-ethyladenine molecularly imprinted polymer

Urban Skogsberg [a], Christoph Meyer [a], Jens Rehbein [a], Gerd Fischer [a], Siri Schauff [a], Norbert Welsch [a], Klaus Albert [a], Andrew J. Hall [b], Börje Sellergren [b,*]

[a] *Institute of Organic Chemistry, University of Tuebingen, Auf der Morgenstelle 18, 72076 Tuebingen, Germany*
[b] *Institut für Umweltforschung, Universität Dortmund, Otto Hahn Strasse 6, 44227 Dortmund, Germany*

Received 23 July 2006; received in revised form 24 October 2006; accepted 30 October 2006
Available online 20 November 2006

Abstract

Suspended-state high resolution/magic angle spinning nuclear magnetic resonance spectroscopy and solid-state cross-polarization/magic angle spinning nuclear magnetic resonance spectroscopy were employed to study the interactions between 9-ethyladenine and a 9-ethyladenine molecularly imprinted polymer, and a non-imprinted polymer, respectively, both are copolymers of methacrylic acid and ethyleneglycol dimethacrylate. Template-related structural differences between the materials were revealed by contact time measurements and solid-state nuclear magnetic resonance. Rebinding of the template to the imprinted polymer resulted in shorter contact times for nuclei believed to be involved in the binding site interactions whereas the non-imprinted polymer did not exhibit such effects. This indicates that binding site reoccupation has a stiffening effect lowering the mobility of nearby nuclei. More detailed information was obtained from suspended-state saturation transfer difference high resolution/magic angle spinning nuclear magnetic resonance experiments. These revealed molecular level details concerning the interactions of the adenine guests with the polymer binding sites. Thus, a relatively larger transfer of magnetization was observed in the solute when bound to the molecularly imprinted polymer at a position where multiple hydrogen bonds between the analyte and the template can be expected to take place in the molecularly imprinted polymer only.

Keywords: Imprinted polymer; Solid-state NMR; Suspended-state NMR

1. Introduction

The importance of molecularly imprinted polymers (MIPs) as selective chromatographic sorbents or solid phase extraction materials is well documented [1–3]. While they have been successfully applied in these areas, the molecular basis of their ability to discriminate between related molecules is still not fully understood [4].

Knowledge about the interactions taking place between a MIP and a target molecule is of fundamental interest in order to take full advantage of the potential of these materials. Nuclear magnetic resonance (NMR)-techniques are very attractive in this regard, as they provide useful information at a molecular level. Among these, solid-state magic angle spinning (MAS) NMR spectroscopy may be used to reveal information about the structure of a solid sample. For example, NMR is a well-established method to evaluate chromatographic sorbents [5]. Due to low sensitivity and relatively broad signals, this technique has been found to be of limited use in the characterization of the low abundant binding sites present in imprinted polymers [6]. Thus, the examples reported to date describe templates bound to the MIP by strong non-covalent [7] or reversible covalent interactions [8,9]. In these cases the concentration of sites is sufficient to produce

* Corresponding author. Tel.: +49 231 7554082; fax: +49 231 7554084.
E-mail address: b.sellergren@infu.uni-dortmund.de (B. Sellergren).

0032-3861/$ - see front matter © 2006 Elsevier Ltd. All rights reserved.
doi:10.1016/j.polymer.2006.10.036

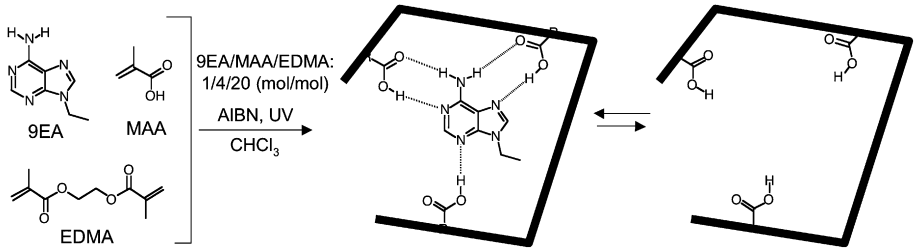

Fig. 1. Procedure followed for the preparation of 9-ethyladenine (9EA) molecularly imprinted polymer (MIP). A control non-imprinted polymer (NIP) was synthesized in the same manner, but with omission of the template.

signals that can be ascribed to interactions involving the templated sites alone. However, solid-state NMR has so far failed in delivering binding site structural information at the molecular level.

One drawback of solid-state NMR is that mechanistic studies of the interactions occurring between the solid phase and an analyte are precluded due to the absence of solvents. Recently, studies on the interactions between an analyte dissolved in a mobile phase and a solid chromatographic sorbent were reported via the use of suspended-state high resolution/magic angle spinning (HR/MAS) NMR spectroscopy [10–13]. The obtained NMR data were successfully correlated with the chromatographic performance, showing the usefulness of sophisticated NMR techniques such as nuclear Overhauser effect spectroscopy (NOESY) and rotation frame Overhauser effect spectroscopy (ROESY) to elucidate chromatographic retention mechanisms. Thus, important information could be obtained to describe the nature of the interactions occurring between the sorbent and the analyte.

Solution-state NMR on the other hand is widely used to map atom–atom distances within a molecule, as well as between molecules. Therefore, NMR has often been used to study interactions taking place between dissolved portions of a stationary phase and analytes in solution in order to extract information about retention mechanisms taking place in high performance liquid chromatography (HPLC) [14,15]. Furthermore, it has been used to gain information concerning the strength of such interactions. Several solution-state NMR studies have been performed to determine the association constant (K_a) between the MIP precursor monomers and the template to decide which monomer is most suitable for the synthesis of a new MIP [6,16–21]. Moreover, these predicted monomer–template complexes are believed to reflect the structure of the binding sites subsequently formed during polymerization. However, this model is still hypothetical and lacks supporting evidence from direct characterization of the polymer binding sites at a molecular level.

In order to obtain information about the interactions between an analyte and a sorbent by suspended-state HR/MAS NMR, an exchange of the analyte between the solvent and the sorbent that is rapid on the NMR time scale is required. For instance, if the analyte interacts too strongly, the signals will suffer excessive broadening and will have a low informative value. Due to the heterogeneous distribution of binding sites in most MIPs, the interactions between a MIP and an analyte can take place in a number of manners [22]. In some cases, this distribution can be modeled by a Langmuir binary site model involving one class of high energy sites of low abundance and one class of more abundant low energy sites. Thus, binding in such systems involves both rapidly and slowly exchanging sites on the NMR time scale [23].

By combining solid-state MAS NMR spectroscopy, giving information concerning the strong interactions where the analyte is adsorbed, and suspended-state HR/MAS NMR for probing the weaker interactions where the exchange is rapid, a more complete picture of the nature of the imprinted sites and of the interactions with an analyte may be obtained. For this purpose we have here made use of these tools for the characterization of a polymer imprinted with 9-ethyladenine (9EA) (Fig. 1).

9EA has been extensively used as a model template for a MIP showing pronounced affinity and selectivity for adenine containing targets [24]. Equilibrium partitioning experiments demonstrated that the isotherms describing the binding of 9EA to a 9EA MIP in chloroform could be fitted well using a Langmuir binary site model comprising one class of high energy sites ($N = 20$ μmol/g, $K_a = 77\,000\ M^{-1}$) and one class of low energy non-selective sites (53 μmol/g, $K_a = 2400\ M^{-1}$). The structure of the high energy sites was proposed based on a detailed solution-state NMR study of butyric acid interacting with 9EA [25]. This involved complexes (Scheme 1)

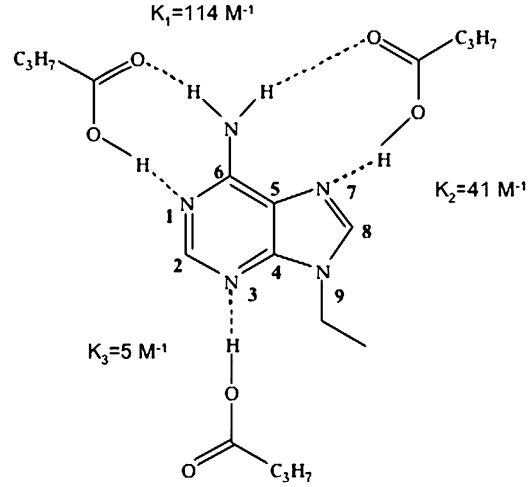

Scheme 1.

where each 9EA molecule is complexed up to three butyric acid molecules with a net binding constant of 160 M^{-1}. Previously, we have studied this model system with the objective of understanding the process of binding site formation in MIPs [26]. The conversion of the individual monomers and the monomer–template interactions could then be monitored with time by ^{1}H NMR in an in situ curing experiment. A pronounced broadening of the template signals precluded any information to be gained concerning the template microenvironment after macrogelation had occurred.

Using the strategy of combining the various NMR techniques described above we hoped to obtain more information in this regard and be able to conclude whether the solution complexes are translated into the polymer through the templating process.

2. Experimental

2.1. Materials

The monomers, methacrylic acid (MAA) and ethyleneglycol dimethacrylate (EDMA) were obtained from Aldrich Chemical Company Inc. (Milwaukee, WI, USA) and purified prior to use to remove residual inhibitor molecules according to the following procedures. MAA was distilled under reduced pressure. EDMA was washed consecutively with aqueous 10% NaOH solution. After drying over $MgSO_4$, it was filtered and distilled under reduced pressure. $CHCl_3$ was obtained from Fluka (Buchs, Switzerland), and dried prior to use to remove the traces of water by passing over silica gel (14 mL $CHCl_3$ per 10 g silica). *N*,*N*′-Azo-bis-isobutyronitrile (AIBN) was obtained from Acros Organics (Geel, Belgium) and recrystallised from methanol before use. Adenine-8-^{13}C-6-amino-^{15}N-1-^{15}N-9-^{15}N (^{13}C, 92.5%; 6-amino-^{15}N, 80%; 1-^{15}N, 20%; 9-^{15}N, 98%) was obtained from Cambridge Isotope Laboratories, Inc., (Andover, USA). $CDCl_3$ (99.8%) (Merck, Darmstadt, Germany) was stored over molecular sieves. C_6D_{12} (99%) and CD_3OD (99.8%) (Merck, Darmstadt, Germany) were used from freshly opened vials. 9EA was synthesized in-house from adenine and ethyl bromide as described previously [25].

2.2. Polymer synthesis

The synthesis of the 9EA MIP was performed according to the following template polymerization procedure modified from the literature [24]. MAA (4 mmol), EDMA (20 mmol) and AIBN (1% w/w of total monomers) as initiator, were added to a solution of 9EA (1 mmol) in 5.6 mL $CHCl_3$. The polymerization was performed in a sealed glass tube, initiated thermally at 333 K, and allowed to proceed at this temperature for 24 h. Afterwards, the polymerization tube was broken and the polymer monolith was removed. After crushing, template molecules and unreacted monomers were removed by extraction with methanol in a Soxhlet apparatus for 24 h. Thereafter, the polymer was crushed further and sieved to yield particles of the desired size (25–36 μm). The splitting yield was determined by analysis of the extracts by chromatography. The control non-imprinted polymer (NIP) was prepared using the same procedure, but without the template molecule 9EA.

2.3. Binding experiments

Adenine-8-^{13}C-6-amino-^{15}N-1-^{15}N-9-^{15}N (6.9 mg) was dissolved in a solvent mixture (50 mL) composed of acetonitrile (70%) and potassium phosphate buffer (0.02 M), adjusted to pH = 3.2 (30%), to yield a concentration of 1 mM. Six different volumes of adenine solution were added to different Erlenmeyer flasks (10 mL, 5 mL, 2.5 mL, 1.25 mL, 0.625 mL and 0.313 mL). The volume in each flask was adjusted to 10 mL with the acetonitrile/phosphate buffer solution. MIP or NIP (120 mg) was added to each flask and shaken gently for 24 h at room temperature. After filtration, the polymers were dried and stored in a desiccator over P_2O_5 for 96 h.

The MIP suspension for the contact time variation experiments was prepared according to the following procedure. MIP (300 mg) was incubated with 12 mL of a solution of 9EA in chloroform (0.1 mM). The incubation mixture was shaken gently overnight at room temperature. After filtration and washing, the incubated MIP was dried and stored in a desiccator over P_2O_5 for 96 h. The same procedure was used to rebind non-labeled adenine to the MIP, except that the adenine was dissolved in a solvent composed of acetonitrile (70%) and potassium phosphate buffer (0.02 M), adjusted to pH = 3.2 (30%).

2.4. Solid-state ^{13}C cross-polarization/magic angle spinning (CP/MAS) NMR

All ^{13}C CP/MAS NMR spectra were recorded on a Bruker ASX 300 spectrometer (300 MHz, 7.05 T) at a spinning rate of 10 000 Hz with 4 mm double bearing rotors of ZrO_2. The proton 90° pulse length was 3.5 μs and the temperature was 295 K. The spectra were obtained with a cross-polarization contact time of 3 ms and the pulse intervals were 2–300 s. TMS was used as a reference to adjust the ^{13}C ppm scale whereas glycine was used as a reference to adjust the Hartmann–Hahn condition. The number of transients recorded in each experiment was 20 480. However, due to the rigid crystalline structure of adenine, surprisingly long pulse intervals were needed to allow complete spin relaxation. We found that the optimal delay time was 5 min. The measurements in this case were stopped after 900 scans.

2.5. Solid-state ^{15}N CP/MAS NMR

All ^{15}N CP/MAS NMR spectra were recorded on a Bruker ASX 300 spectrometer (300 MHz, 7.05 T) at a spinning rate of 10 000 Hz with 4 mm double bearing rotors of ZrO_2. The proton 90° pulse length was 3.5 μs and the temperature was 295 K. The spectra were obtained with a cross-polarization contact time of 5.5 ms and the pulse intervals were 2 s. ^{15}N enriched ammonium nitrate was used as a reference and glycine

was used to adjust the Hartmann–Hahn condition. The number of transients recorded in each experiment was 32 000.

2.6. Suspended-state HR/MAS NMR titration experiments

All NMR spectra were referenced to the residual $CHCl_3$ peak at 7.26 ppm. All suspended-state HR/MAS NMR spectra were recorded on a Bruker 400 MHz spectrometer at a spinning rate of 4500 Hz with 4 mm double bearing rotors of ZrO_2. Each rotor contained 60 μL of the corresponding stock solution and different amounts of MIP or NIP. For each spectrum a minimum of 512 transients were recorded. In order to guarantee a sufficient signal to noise ratio when a lower concentration of analyte was used, up to 4096 transients were recorded. The 90° pulse was set to 8.5 μs. The analyte was dissolved in $CDCl_3$ at different concentrations and added to the polymer with a syringe. All spectra were recorded at 300 K.

Stock solutions for the suspended-state HR/MAS NMR experiments were prepared by dissolving 9EA (1.28 mg) in $CDCl_3$ (0.75 mL) ([9EA] = 10.4 mM), 9EA (1.29 mg) in 33% CD_3OD (0.25 mL) in $CDCl_3$ (0.50 mL) ([9EA] = 10.5 mM) or 9EA (1.18 mg) in 20% C_6D_{12} (0.15 mL) in $CDCl_3$ (0.60 mL) ([9EA] = 9.65 mM).

2.7. Suspended-state STD HR/MAS NMR experiments

All suspended-state STD HR/MAS NMR spectra were recorded on a Bruker 400 MHz spectrometer at a spinning rate of 4500 Hz with 4 mm double bearing rotors of ZrO_2. For each suspended-state STD HR/MAS experiment, 6.0 mg of either MIP or NIP was suspended in 80 μL of the corresponding stock solution. In each experiment, a total of 8192 transients were recorded. The 90° pulse was set to 8.5 μs. A delay of 2 s was used before a new transient was recorded and the acquisition time was 3.3 s. All spectra were recorded at 300 K.

3. Results and discussion

The 9EA MIP and the control NIP were synthesized from MAA and EDMA as described in Section 2. Overnight extraction of the ground polymers in a Soxhlet apparatus using methanol as solvent resulted in the removal of more than 94% of the added template, indicating the presence of a large number of accessible binding sites.

Comparing the solid-state ^{13}C CP/MAS NMR spectra of the MIP (i) and NIP (ii), no differences in the chemical shifts or relative signal intensities can be seen, indicating that the materials were chemically equivalent (Fig. 2). All signals could be assigned in agreement with the expected composition of the polymers and taking into account a small portion (approximately 10%) [4] of unreacted double bonds (signals at $\delta = 125$, 138 and 168 ppm).

In order to investigate the higher energy imprinted sites and how the binding responded to the polarity of the solvent, the materials were first incubated with different concentrations of 9EA in different solvents. Peak integrals with reference to an internal standard allow for the indirect calculation of the amount of analyte bound to the polymers. Assuming the peak area of the non-adsorbed internal standard to be constant, the ratio between the internal standard and 9EA peak integrals will reflect how much 9EA is bound to the polymers.

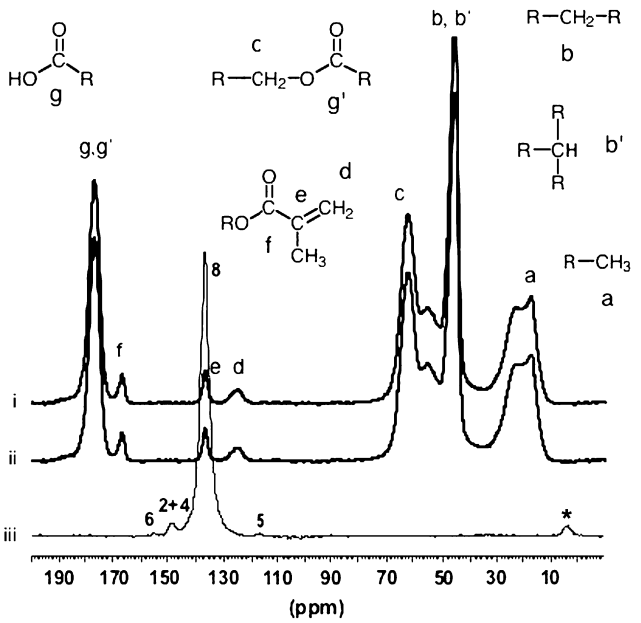

Fig. 2. Solid-state ^{13}C CP/MAS NMR spectra of the (i) MIP, (ii) NIP, and (iii) labeled adenine (adenine-8-^{13}C-6-amino-^{15}N-1-^{15}N-9-^{15}N).

The use of aprotic solvents for solvation of the analytes resulted in pronounced differences in the adsorption isotherms of the MIP and NIP, with a considerably larger uptake of 9EA (approximately 50 μmol/g) displayed by the MIP (Fig. 3). This is in agreement with a previous report and points to an approximately 25% yield of the imprinted high energy binding sites in the polymer [24].

However, in spite of the strong uptake of template, the solid-state ^{13}C CP/MAS NMR spectra of the incubated samples showed no signals corresponding to bound 9EA. This is presumably due to pronounced signal broadening caused by reduced mobility of the template when bound to the polymer [26]. It is known that quantification of functional groups in solids based on solid-state NMR signal intensities is not directly possible due to the cross-polarization effect [27,28]. The build-up of ^{13}C magnetization is carried out in a definite contact period in which the energy levels of abundant ^{1}H and rare ^{13}C spins are identical. The build-up of ^{13}C magnetization (I) then occurs at a rate defined by the cross-relaxation constant, T_{CH}, whereas the falloff is a result of the decrease in the spin-locked ^{1}H magnetization, which decays with the proton spin–lattice relaxation time in the rotating frame, $T_{1\rho}$, according to Eq. (1) [28].

$$I(t) = I_0(1 - T_{CH}/T_{1\rho})^{-1}[\exp(-t/T_{1\rho}) - \exp(-t/T_{CH})] \quad (1)$$

T_{CH} is dependent on the distance between protons and ^{13}C nuclei, as well as their mobility; highly flexible molecules need a longer time compared to more rigid molecules. This means,

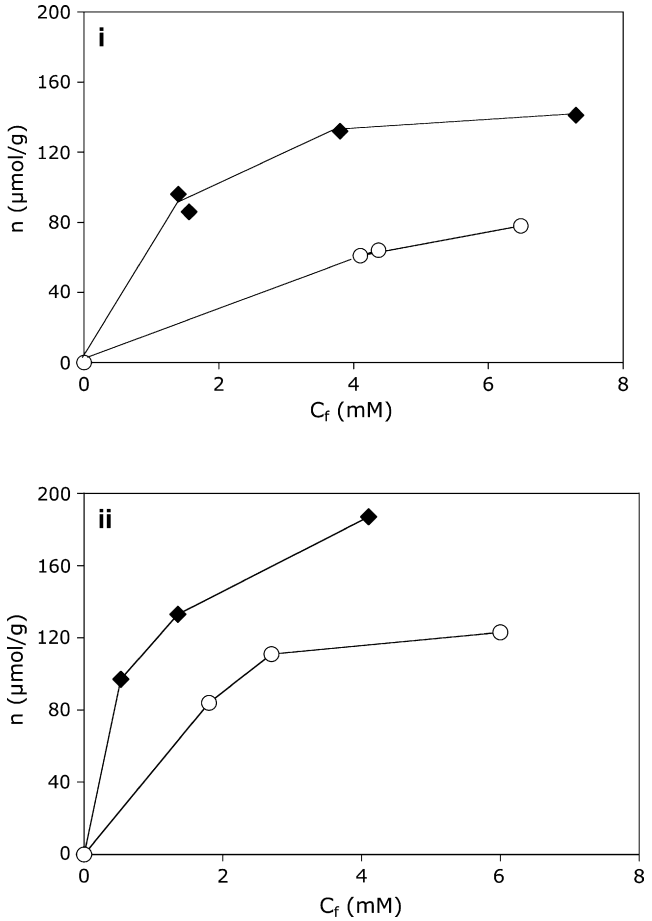

Fig. 3. Binding isotherms showing adsorbed amounts (n) of 9EA by the MIP (filled diamonds) and NIP (open circles) calculated from the suspended-state HR/MAS NMR experiments using $CHCl_3$ as internal standard. The rotor contained 64 µL of a stock solution of 9EA (10.4 mM) in (i) $CDCl_3$ and (ii) $CDCl_3/C_6D_{12}$ (80/20 v/v), respectively, to which different amounts of polymer were added. The expected maximum capacity of the polymers would be 240 µmol/g if all templates gave rise to an accessible site. The amount of bound 9EA was calculated from the signal integral in absence of added polymer and in the presence of increasing amounts of polymer (1.4, 3.2, 6.0, 6.6 mg) after equilibration for 24 h.

in principle, that every single carbon in a molecule has an individual contact time that will give the maximum signal enhancement in the CP/MAS NMR spectra.

By performing a systematic variation in the contact time, the intensity of a specific signal shows a maximum intensity at a distinct contact time T [29]. A change in T for individual nuclei in compositionally identical materials can be used to indicate changes in their structural mobility and microenvironment. This could be for instance prior to or after an incubation with template. Three different contact time variation experiments were thus performed on the 9EA MIP and the corresponding NIP; incubated with 9EA or adenine. The concentration of 9EA was low (0.1 mM) in order for the analyte to occupy predominantly the high energy sites of the MIP. The experiments were then performed to observe if the two polymers exhibited different T's for a certain signal and whether these contact times were different after the incubation experiment with 9EA or adenine. Since the same MIP and NIP were used in all three experiments, a difference in T for a certain signal can be interpreted as a change in the structural mobility of the corresponding nucleus during incubation. The contact times for each of the signals prior to and after incubation are shown in Table 1. From the experiments with the free polymers (MIP and NIP), the relative order of the contact times when comparing all signals were the same. However, the absolute values were not identical with some signals (a and b) of the MIP exhibiting longer contact times and some (e and f) shorter in relation to those of the NIP. The olefinic carbon (e) of the pendent double bonds and the corresponding carbonyl group (f) at $\delta = 167$ ppm, show relatively long T's with the NIP slightly exceeding the MIP. This reflects the low number of vicinal protons attached to these nuclei and indicates that those of the MIP are somewhat more restricted in their mobility.

Table 1
Contact times at maximum signal intensity T (ms) for the ^{13}C chemical shifts (ppm), determined from contact time variation curves, of the void MIP, MIP incubated with adenine (0.1 mM in acetonitrile/phosphate buffer (70/30 v/v) at a pH 3.3), and MIP incubated with 9EA (0.1 mM in $CHCl_3$); (signal d was not considered here)

Peak	a	b	c	e	f	g
Chemical shift (ppm)	18	45	62	137	167	177
MIP	3.1	2.2	1.1	6.4	6.0	3.2
MIP incubated with adenine	2.9	3.1	0.9	3.0	6.0	3.3
MIP incubated with 9EA	1.5	2.0	1.2	3.1	5.1	2.2
NIP	2.2	1.7	1.3	9.1	7.7	3.0
NIP incubated with adenine	2.1	1.6	1.7	10.5	7.4	2.8
NIP incubated with 9EA	2.4	1.9	1.3	10.8	7.7	3.1

On the other hand the T of the backbone nuclei (a and b) is significantly longer in MIP indicating more mobility in this case. The reason for these differences is far from obvious but it is known that the presence of template leads to morphological differences reflected in pore system related parameters, swelling and pH-titration curves [4]. Moreover, we recently showed that 9EA affects the onset of polymerization of the MAA–EDMA monomer pair, with a significant retardation observed in the presence of template. A slower incorporation of MAA into the MIP could possibly account for the pendents residing in more crosslinked segments, although no such effect was observed [26].

For the MIP incubated with either adenine or 9EA, significantly shorter T's were observed for signal e at $\delta = 137$ ppm, (Fig. 4) and signal a at $\delta = 18$ ppm. In the latter case only 9EA gave rise to a shorter contact time. These differences are likely due to overlapping of the analyte signals C-8 ($\delta = 137$ ppm) in adenine and 9EA as well as the ethyl group ($\delta = 18$ ppm) present in 9EA with the polymer signals. Nevertheless, the absence of such effects in the NIP confirms that solutes are occupying imprinted sites in the MIP.

The T for the carbonyl signal at $\delta = 177$ ppm, corresponding to the carboxylic acid and ester carbonyls, is shortened

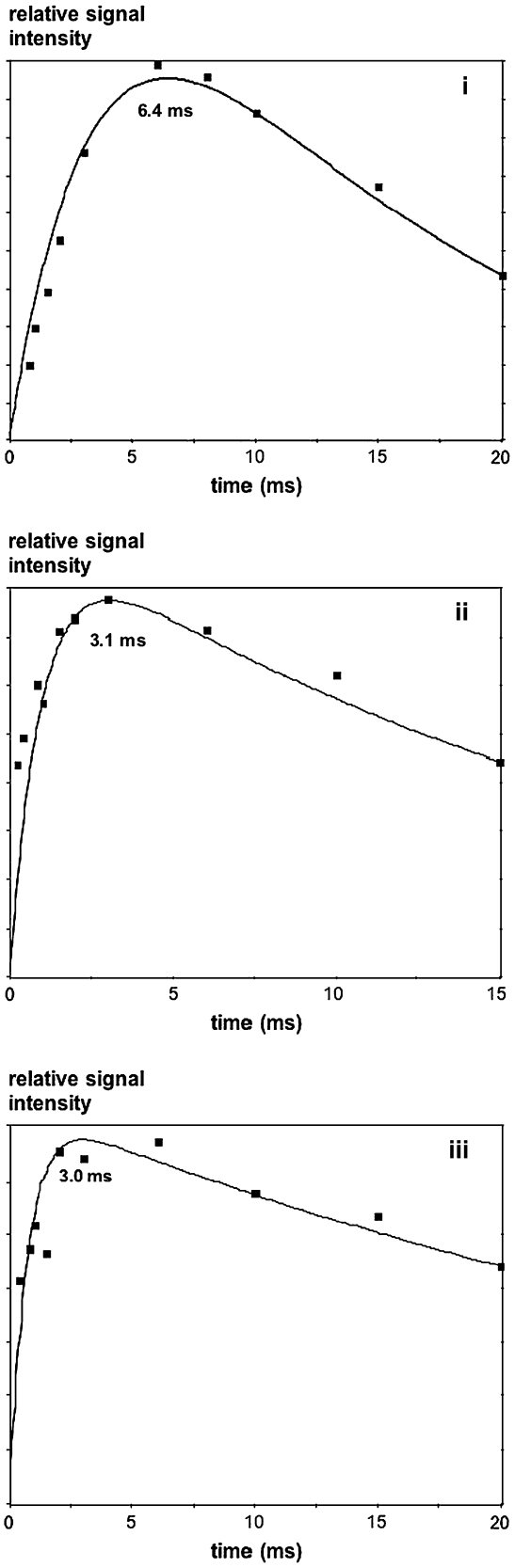

Fig. 4. Contact time variation curves of the carbon chemical shift signal e at 137 ppm: (i) MIP, (ii) MIP incubated with 9EA, and (iii) MIP incubated with adenine.

from 3.2 ms to 2.2 ms for the MIP incubated with 9EA. This indicates a restricted mobility of these groups, most probably due to hydrogen bond interactions involving the carboxylic acid groups and 9EA. A weaker effect was observed for signal f at $\delta = 167$ ppm, which dropped from 6.0 ms to 5.1 ms after incubation with 9EA. Interestingly, none of the above signals experienced a change in T upon contact with adenine. This reflects the higher affinity of the MIP for 9EA compared to adenine [24].

From the above results we concluded that a ^{13}C- or/and ^{15}N-labeled compound was needed to obtain a sufficient signal to noise ratio in the solid-state CP/MAS NMR experiments of the incubated samples. Therefore, incubation experiments were performed with adenine-8-^{13}C-6-amino-^{15}N-1-^{15}N-9-^{15}N. The ^{13}C CP/MAS NMR spectrum of this probe (Fig. 2iii) shows that the enriched nuclei (C-8) appears with a similar chemical shift as the signal of the double bond (denoted e) of the polymers at $\delta = 137$ ppm. This unfortunate signal overlap makes it considerably more difficult to interpret the position, shape and intensity of the C-8 signal in terms of dynamic and thermodynamic factors related to the binding event. Nevertheless, after incubation of the MIP and NIP, respectively, with different amounts of labeled adenine dissolved in a acetonitrile/phosphate buffer (70/30 v/v) solution at pH 3, solid-state CP/MAS NMR spectra were recorded. A shoulder on the signal at $\delta = 137$ ppm can be observed in the solid-state ^{13}C CP/MAS NMR spectrum of the adenine incubated MIP (Fig. 5a). In order to distinguish between weakly and strongly adsorbed adenine each sample was washed for 2 h with the acetonitrile/phosphate buffer solvent mixture used for the incubation experiment. Thereafter, all the samples were measured once again. However, after this treatment, the signal at $\delta = 140$ ppm was no longer observed.

Therefore, we assume that the chemical shift position of the shoulder at $\delta = 140$ ppm corresponds to the ^{13}C labeled C-8 position of bound adenine. This was confirmed by performing a further solid-state ^{13}C CP/MAS NMR experiment, with a different contact time, with the adenine-incubated MIP. By choosing a shorter contact time (0.1 s), it was possible to change the ratio of the two signal areas at $\delta = 137$ ppm (which was reduced), and 140 ppm (which was then increased), thus confirming that two separate signals were present (Fig. 5b). The peak maximum at $\delta = 140$ ppm of bound adenine indicates a chemical shift displacement of approximately 2 ppm downfield compared to the peak observed for crystalline adenine ($\delta = 138$ ppm). Such shifts are in agreement with the deshielding effects which can be expected due to the hydrogen bonds known to be present involving N-7 in adenine (Scheme 1). No C-8 signal was observed after incubating the polymers in solutions of concentrations lower than 0.25 mM.

The materials incubated with 1 mM solutions of adenine (see above) were further investigated by solid-state ^{15}N CP/MAS NMR spectroscopy. Due to the absence of nitrogen in the polymer matrix, only template-related peaks appear in these spectra (Fig. 6). No signal can be observed for the adenine N-1 due to the low isotopic labeling (20%), but the

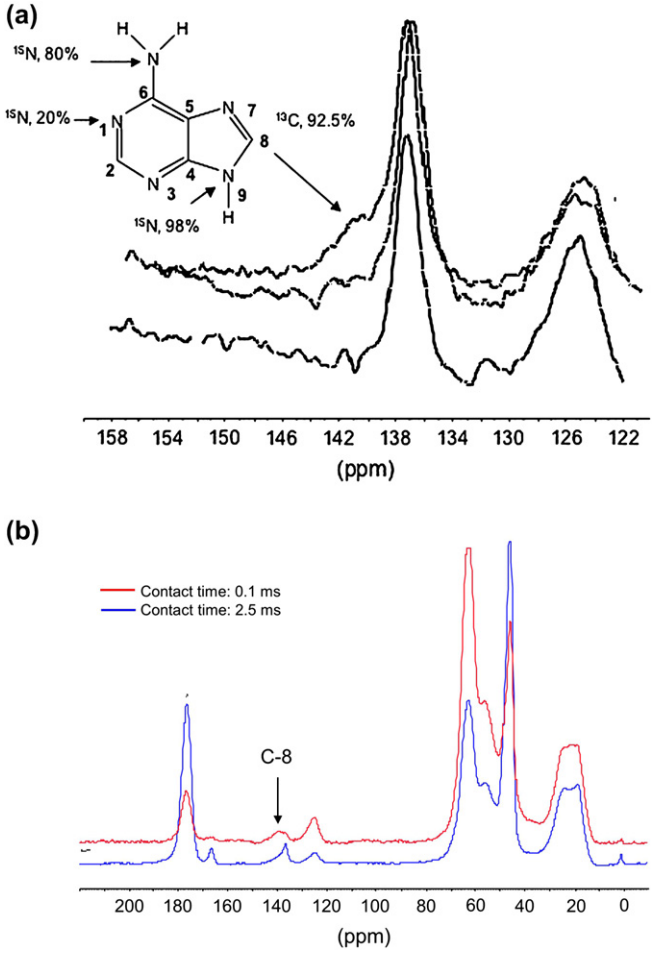

Fig. 5. (a) Solid-state ^{13}C CP/MAS NMR spectra of the MIP after incubation with labeled adenine (upper spectrum), before incubation (middle spectrum) and after washing with acetonitrile/phosphate buffer solution (lower spectrum), and (b) of the MIP after incubation with labeled adenine at different contact times.

signals corresponding to N-6 and N-9, with a higher isotopic labeling, appear in the spectra (80 and 98%, respectively).

When comparing the chemical shifts of the signals (Table 2), significant differences were observed for bound, free or crystalline adenine. First, the chemical shift positions for signals N-6 and N-9 are changed when adenine is adsorbed by the MIP and the NIP.

From a comparison of the ^{15}N solid-state CP/MAS spectra of crystalline adenine and polymer-bound adenine (for both MIP and NIP), an upfield shift of approximately 12 ppm is observed for N-6. This, in turn, corresponds to a position approximately 20 ppm downfield from the chemical shift of N-6 of free adenine in solution (solution preparation as described in Section 2). On the other hand, the N-9 signal of adenine bound to the MIP exhibits a less dramatic change in chemical shift, at $\delta = 152$ ppm, which is comparable to the chemical shift of the N-9 signal of adenine in solution ($\delta = 149$ ppm). Contrary to this, the signal at $\delta = 163$ ppm for the N-9 of adenine bound to the NIP is closer to the signal ($\delta = 163$ ppm) of the N-9 of crystalline adenine ($\delta = 159$ ppm). These shift changes are likely due to different hydrogen bond interactions between

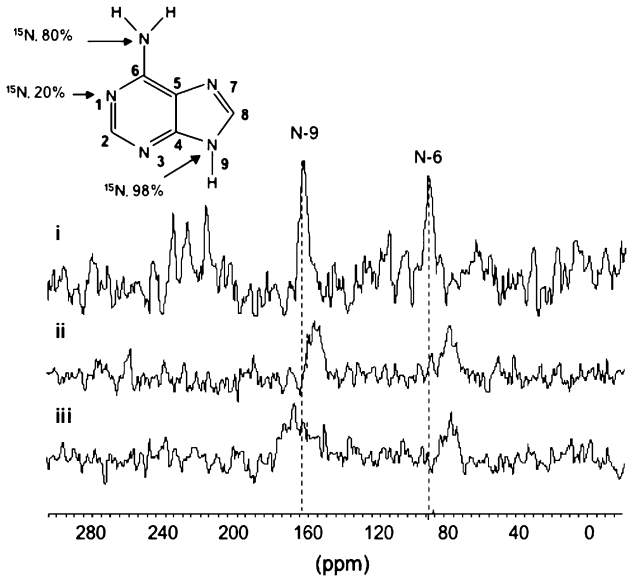

Fig. 6. Solid-state ^{15}N CP/MAS NMR spectra of: (i) free adenine, (ii) MIP after incubation with labeled adenine, and (iii) NIP after incubation with labeled adenine.

adenine and the medium in which it is present [30]. It is known that the protonation of adenosine with trifluoro acetic acid in dimethylsulfoxide results in a downfield shift of N-6 of approximately 7 ppm, from 83 ppm to 90 ppm [31]. Furthermore, it is known that the signal of the nitrogen nucleus of amino groups in molecules like imidazoles experiences an upfield shift due to the abstraction of the proton attached to the nitrogen while interacting via a hydrogen bond.

Hence, the downfield shift of N-6 observed for bound adenine compared to free adenine indicates that an interaction with the carboxylic acid groups is present. Since no significant difference is observed between the chemical shifts of N-6, the magnitude of the hydrogen bond appears to be similar for the MIP and the NIP. Concerning N-9 on the other hand, the high shift of the MIP and the low shift of the NIP may reflect the presence of an accepting site in the MIP that is absent in the NIP. This would agree with a binding site model where each adenine is complexed by three acid groups in the site (Scheme 2). Also, significant differences in the ^{15}N signal widths were observed, as seen in Fig. 6. Thus, the NIP exhibited broader N-9 and N-6 signals than the MIP, although the band positions of N-6 were comparable.

This may indicate that adenine bound to the NIP experiences a larger variety of sites than that of adenine bound to the MIP, where the sites occupied appear to be more homogeneous.

Table 2
Comparison of the ^{15}N chemical shifts (ppm) of labeled adenine in different chemical environments

Condition	N-6	N-9
Crystal	89.1	158.7
Solution	57.1	148.7
Bound to MIP	76.8	151.8
Bound to NIP	76.3	163.2

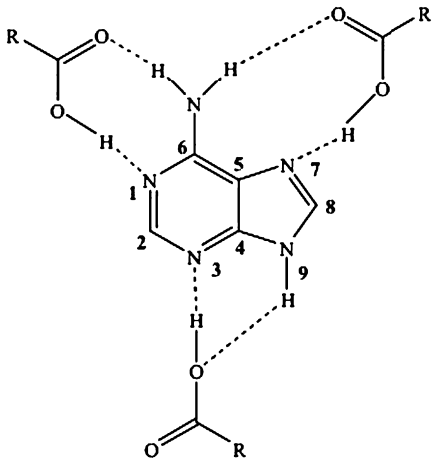

Scheme 2.

After washing the incubated MIP and NIP with the acetonitrile/phosphate buffer solution used in the rebinding experiments, no signals were observed in the solid-state ^{15}N CP/MAS NMR experiment. This indicates that adenine was weakly adsorbed to the polymers under these conditions and the low sensitivity precluded the detection of strongly bound adenine in the ^{15}N NMR measurements. No signals were observed, neither before nor after the wash step, when these experiments were repeated using chloroform/methanol (80/20 v/v) as solvent for the incubation experiments. This indicates that the probe is even more strongly bound under these conditions.

We thereafter turned to suspended-state ^{1}H HR/MAS NMR to investigate whether this technique could reveal differences between the materials that could be ascribed to templated sites. Thus, the interactions of 9EA with the polymers in chloroform, as well as in mixtures of chloroform with methanol or cyclohexane, were studied. The strong interactions taking place between 9EA and the high affinity sites of the MIP ($K_a = 77\,000\ M^{-1}$) imply that little or no exchange of free and strongly bound 9EA takes place. Thus, this technique detects the free 9EA in solution, which interacts relatively weakly with the polymers in the magnitude of $10-1000\ M^{-1}$ and hence is limited to probing sites of lower energy. The downfield shift observed for the amino group (H-12) at $\delta = 5.5$ ppm indicates that 9EA interacts with both MIP and NIP (Fig. 7).

From the spectra in Fig. 7, it is obvious that the peak at $\delta = 5.5$ ppm, corresponding to H-12, was shifted significantly downfield when MIP or NIP was added to the 9EA solution. The peak continued to shift upon further additions of polymer, leveling off at a $\Delta\delta$ of ca. +1.5 ppm for both MIP and NIP after adding approximately 6 mg of polymer. The downfield shift shows that the change in the chemical environment to a more electron rich surrounding of the H-12 protons is caused by hydrogen bonding between the polymer and 9EA [25,32]. The continued downfield shift indicates that the equilibrium between 9EA and the polymer in the free and bound forms is shifted towards the polymer-bound form. No chemical shift movements were observed for the signals H-8, H-2, H-10 and H-11.

The similar behavior of the MIP and NIP indicates that the chemical shift movements of the NMR signal H-12 are due to

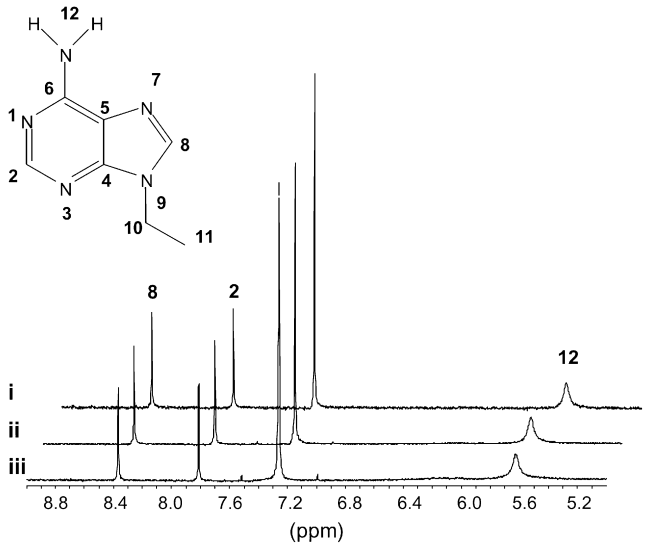

Fig. 7. Suspended-state HR/MAS NMR spectra of: (i) 9EA dissolved in $CDCl_3$ (10.4 mM), in the presence of (ii) MIP (3.2 mg), and (iii) NIP (3.2 mg).

non-specific interactions of the same magnitude. An STD NMR experiment allows one to gain information concerning which protons of a bound species are located in closest contact with the binding site of a receptor [23]. Therefore, liquid-state STD NMR spectroscopy is a common screening technique for protein–ligand interactions [33,34]. Moreover, this technique has been used to observe binding affinities in heterogeneous samples by applying HR/MAS NMR [35].

The principle behind this technique applied to the system described here is as follows. Magnetization from the polymer can be transferred to free 9EA if a selective *on-resonance* pulse is performed. This pulse is placed where only the protons from the polymer are saturated and not the protons in the 9EA. Then, due to spin-diffusion, all the protons in the polymer will be saturated. The broad signals of the insoluble polymer present in the suspended-state HR/MAS NMR spectra make it possible to place the *on-resonance* pulse at $\delta = -1$ ppm, a frequency where no signals from the free 9EA are saturated. However, if 9EA is associated with the polymer, magnetization will be transferred from the protons in the polymer to the interacting protons in 9EA. Due to exchange of free and bound 9EA, magnetization will be transferred to 9EA in solution. Then a second pulse is performed which is *off-resonance*. This pulse is placed where no signals are observed, here at $\delta = 20$ ppm. This experiment corresponds to a normal suspended-state HR/MAS NMR spectrum of the polymer suspension. By subtracting the *on-resonance* experiment from the *off-resonance* experiment, a suspended-state STD HR/MAS NMR spectrum is obtained. Here, one can observe only 9EA signals, which have been enhanced by the magnetization transfer. Hence, this reflects which protons in 9EA are located in closest contact with the binding sites of the MIP or NIP.

Fig. 8a shows the suspended-state ^{1}H HR/MAS NMR spectrum (i) and the suspended-state STD HR/MAS NMR spectrum (ii) of the MIP. Differences in the peak areas can be observed.

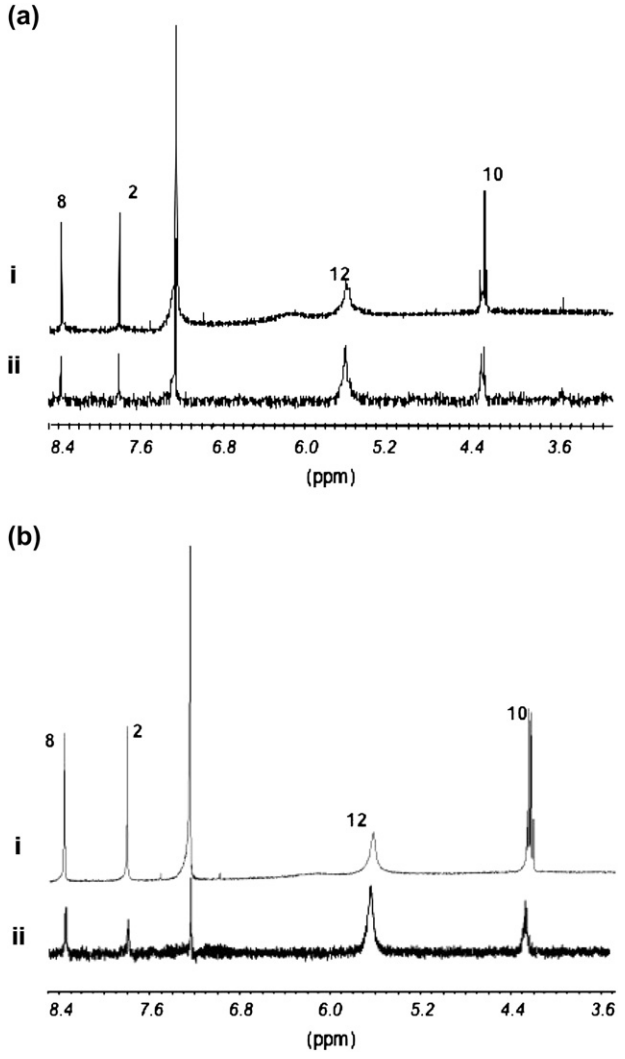

Fig. 8. (a): (i) Suspended-state ^{1}H HR/MAS NMR spectrum of 9EA dissolved in $CDCl_3$ (10.4 mM) in the presence of MIP (6.0 mg), (ii) suspended-state STD HR/MAS NMR spectrum of 9EA dissolved in $CDCl_3$ (10.4 mM) in the presence of MIP (6.0 mg). (b): (i) Suspended-state ^{1}H HR/MAS NMR spectrum of 9EA dissolved in $CDCl_3$ (10.4 mM) in the presence of NIP (6.0 mg), (ii) suspended-state STD HR/MAS NMR spectrum of 9EA dissolved in $CDCl_3$ (10.4 mM) in the presence of NIP (6.0 mg).

Signal enhancements corresponding to the protons H-8, H-2, H-12 and H-10 are observed in the STD spectrum, showing that magnetization is transferred to these protons. However, the signal corresponding to H-12 shows largest significant signal enhancement in the STD NMR experiment. This shows that the major interaction between 9EA and the MIP takes place *via* the amino group in 9EA. The same applies to the NIP, although not to the same extent (Fig. 8b). More details concerning this interaction were derived from the relative enhancements of the different protons (see below). The relative enhanced signal intensities obtained from the suspended-state STD HR/MAS NMR experiment of 9EA in the presence of either MIP or NIP are presented in Table 3. All signal intensities were normalized to the signal corresponding to the most enhanced signal (that is H-12), which was set to 100%.

Table 3
Relative integrals (%) calculated from the integrals obtained in the suspended-state STD HR/MAS NMR experiment of 9EA dissolved in $CDCl_3$ in the presence of MIP or NIP. The signal showing the highest signal enhancement was set to 100%

Signal	In presence of MIP	In presence of NIP
H-8	7	13
H-2	14	7
H-12	100	100
H-10	29	33

Comparing the relative enhancements, the signals corresponding to H-2 are more enhanced than that of H-8 if the MIP is added to the stock solution whereas the opposite is true when the NIP is added. This implies that 9EA forms a closer contact with the MIP binding sites at H-2 but not in the NIP. Since protons H-2 and H-8 in 9EA are located far from each other and surrounded by different nitrogens, the difference in transfer of magnetization to H-2 and H-8 may reflect the relative contributions of the different hydrogen bonds depicted in Scheme 1, on one hand involving N-1 and N-3 (affecting H-2) or on the other hand N-7 (affecting H-8). As seen in Scheme 1, the Watson–Crick type hydrogen bond is the most stable of these interactions, followed by the Hoogsteen type and, finally, the single hydrogen bond to N-3. Assuming the binding constants for the pre-polymerization mixture, mass balance equations allow the estimation of the relative populations of the different complexes. Thus, a significant amount of the higher complexes, 1:2 and 1:3, are believed to be present prior to polymerization. Assuming further that these complexes are stable during polymerization, the MIP is believed to contain sites roughly reflecting the solution complex distribution, whereas the NIP mainly contains sites with only one carboxylic acid group.

Hence, the intensity difference in the STD NMR experiment may reflect the presence of binding sites reflecting an arrangement of carboxylic acid groups interacting with both N-1 and N-3 of 9EA (Scheme 1). This would provide an explanation to the relatively larger enhancement of H-2 in the MIP.

A series of experiments were also performed using solvent mixtures of lower or higher polarity. Thus, when using C_6D_{12} (20%) in $CDCl_3$, considerably more 9EA was adsorbed by both MIP and NIP. This implies that the increase in adsorption is mainly due to an increase in non-specific interactions. Hence, the reduction in polarity of the solvent leads to a reduction in the imprinting effect. The strong overall binding in this solvent system leads to a very low signal to noise ratio, precluding any further conclusions from these experiments to be drawn.

A series of suspended-state HR/MAS NMR experiments were also performed with CD_3OD (33%) added to the $CDCl_3$. Due to hydrogen–deuterium exchange between CD_3OD and the amino group (H-12) in 9EA, no signal corresponding to this group could be observed in the recorded spectra. However, from a comparison of the signal areas (relative to the internal reference $CHCl_3$) obtained in the presence and in absence of MIP, only small changes in peak area ratios were observed, showing that only small amounts of 9EA were adsorbed to the polymers in this solvent system.

4. Conclusions

The solid-state NMR measurements of the ^{13}C-, as well as ^{15}N-labeled analyte, gave valuable information on the different types of binding sites in the imprinted polymers. Template-related structural differences between the materials were revealed by contact time measurements and solid-state NMR. Binding site reoccupation resulted in shorter contact times for nuclei believed to be involved in the binding site interactions. This indicates a lowering of their mobility upon template binding, the template thus acts analogously to a physical cross-linking agent. More detailed information was obtained from suspended-state saturation transfer difference high resolution/magic angle spinning (STD HR/MAS) NMR experiments. These revealed the molecular level details concerning the interactions of the adenine guests with the polymer binding sites. Thus, a relatively larger transfer of magnetization was observed in the solute when bound to the MIP at a position where multiple hydrogen bonds between the analyte and the template can be expected to take place in the MIP only. Together with induced shifts observed in the ^{15}N solid-state NMR experiment, these results support a previously proposed binding site structure involving up to three converging carboxylic acid groups capable of forming complementary hydrogen bonds with adenine containing guests.

Acknowledgements

Brigitte Schindler is appreciated for assistance in performing solid- and suspended-state NMR measurements. We acknowledge the financial support provided through the European Community's Improving Human Potential Program under contract HPRN-CT-2002-00189, [AquaMIP]. C.M., S.S. and G.F. acknowledge the financial support of the Deutsche Forschungsgemeinschaft (Graduiertenkolleg Chemie in Interphasen Grant 441/2), Bonn-Bad-Godesberg.

References

[1] Sellergren B, editor. Molecularly imprinted polymers. Man-made mimics of antibodies and their applications in analytical chemistry, vol. 23. Amsterdam: Elsevier Science BV; 2001.
[2] Andersson LI, Schweitz L. Handbook of analytical separations, vol. 4; 2003. p. 45–71.
[3] Lanza F, Sellergren B. Adv Chromatogr 2001;41:137–73.
[4] Sellergren B, Hall AJ. In: Sellergren B, editor. Molecularly imprinted polymers. Man-made mimics of antibodies and their applications in analytical chemistry, vol. 23. Amsterdam: Elsevier Science BV; 2001. p. 21.
[5] Albert K. J Sep Sci 2003;26:215–24.
[6] Svenson J, Karlsson JG, Nicholls IA. J Chromatogr A 2004;1024: 39–44.
[7] Sasaki DY, Alam TM. Chem Mater 2000;12:1400–7.
[8] Shea KJ, Sasaki DY. J Am Chem Soc 1991;113:4109–20.
[9] Katz A, Davis ME. Nature 2000;403:286–9.
[10] Hellriegel C, Skogsberg U, Albert K, Lämmerhoffer M, Maier NE, Lindner W. J Am Chem Soc 2004;126:3809–16.
[11] Skogsberg U, Händel H, Sanchez D, Albert K. J Chromatogr A 2004; 1023:215–23.
[12] Skogsberg U, Händel H, Gesele E, Sokoliess T, Menyes U, Jira T, et al. J Sep Sci 2003;26:1119–24.
[13] Händel H, Gesele E, Gottschall K, Albert K. Angew Chem Int Ed 2003; 42:438–42.
[14] Yamamoto C, Yashima E, Okamoto Y. J Am Chem Soc 2002;124: 12583–9.
[15] Maier NM, Schefzick S, Lombardo GM, Feliz M, Rissanen K, Lindner W, et al. J Am Chem Soc 2002;124:8611–29.
[16] Sellergren B, Lepistö M, Mosbach K. J Am Chem Soc 1988;110: 5853–60.
[17] Lübke C, Lübke M, Whitcombe MJ, Vulfson EN. Macromolecules 2000; 33:5098–105.
[18] Wulff G, Gross T, Schönfeld R. Angew Chem Int Ed 1997;36:1962–4.
[19] Hall AJ, Achilli L, Manesiotis P, Quaglia M, De Lorenzi E, Sellergren B. J Org Chem 2003;68:9132–5.
[20] Jakusch M, Janotta M, Mizaikoff B, Mosbach K, Haupt K. Anal Chem 1999;71:4786–91.
[21] Dong X, Sun H, Lu X, Wang H, Liu S, Wang N. Analyst 2002;127: 1427–32.
[22] Rampey AM, Rumpleby RJ, Rushton GT, Iseman JC, Shah RN, Shimizu KD. Anal Chem 2004;76:1123–33.
[23] Neuhaus D, Williamson P. The nuclear Overhauser effect in structural and conformational analysis. Weinheim: VCH; 2002.
[24] Shea KJ, Spivak DA, Sellergren B. J Am Chem Soc 1993;115:3368–9.
[25] Lancelot G. J Am Chem Soc 1977;99:7037–42.
[26] Lanza F, Rüther M, Hall AJ, Sellergren B. Mater Res Soc Symp Proc 2002;723:M5.6.1–11.
[27] Colin AF. Solid State NMR for Chemists. Canada: CFC Press; 1983.
[28] Kolodziejski W, Klinowski J. Chem Rev 2002;102:613–28.
[29] Mehring M. In: Diehl P, Fluck E, Kosfeld R, editors. High resolution NMR spectroscopy in solids, vol. 11. New York–Berlin: Springer; 1976. p. 135.
[30] Lorente P, Shenderovich IG, Golubev NS, Denisov GS, Buntkowsky G, Limbach H. Magn Reson Chem 2001;39:S18–29.
[31] Cho BP, Evans FE. Nucleic Acids Res 1991;19:1041–7.
[32] Golubev NS, Denisov GS, Smirnov SN, Shchepkin DN, Limbach H. Z Phys Chem 1996;196:73–84.
[33] Meyer B, Peters T. Angew Chem 2003;115:890–918.
[34] Meyer B, Peters T. Angew Chem Int Ed 2003;42:864–90.
[35] Klein J, Meinecke R, Mayer M, Meyer B. J Am Chem Soc 1999;121: 5336–7.